Brain Imaging and Behavior (2019) 13:1273–1280
https://doi.org/10.1007/s11682-018-9953-6

ORIGINAL RESEARCH

# Multivoxel pattern analysis of structural MRI in children and adolescents with conduct disorder

Jianing Zhang[1] · Wanyi Cao[2] · Mingyu Wang[1] · Nizhuan Wang[1] · Shuqiao Yao[2] · Bingsheng Huang[1,2]

Published online: 25 August 2018


## Abstract

Conduct disorder (CD) is a psychiatric disorder in either childhood or adolescence and is characterized by aggressive and antisocial behavior. Although CD has been shown to be associated with structural abnormalities by structural magnetic resonance imaging (sMRI), the classification ability of these structural abnormalities' spatial patterns remains unclear. The aim of the present study was to characterize these different spatial patterns, which may eventually serve as potential reliable imaging biomarkers in the classification of CD from healthy controls (HCs). High-resolution 3D sMRI was acquired from 60 CD and 60 HCs, and all subjects were male participants. The mean (standard deviation) age was 15.3 (1.0) years old and 15.5 (0.7) years old for the CD and HC group respectively. Multivoxel pattern analysis (MVPA) with searchlight algorithm combined with support vector machine (SVM) was used to characterize the different spatial patterns in grey matter (GM) and to assess the classification ability of such structural difference. Seven cortical and subcortical regions showed significant GM difference between CD and HCs, including the cerebellum posterior lobe, temporal lobe, parahippocampal gyrus, lingual gyrus, insula, parietal lobe and medial frontal gyrus. GM in these brain regions discriminated CD with accuracy of up to 83%. Multiple brain regions exhibited aberrantly different spatial patterns in CD. The spatial patterns might be objective and reliable imaging features that could help to improve the classification of CD.

**Keywords** Conduct disorder · sMRI · Multivoxel pattern analysis · Support vector machine · Classification

## Introduction

CD is a psychiatric disorder in either childhood or adolescence and is characterized by aggressive and antisocial behavior (Fairchild et al. 2011). 8–16% of boys and 3% of girls aged 4–16 years old are diagnosed with CD (Cappadocia et al. 2009). CD is often seen as the precursor to adult antisocial personality disorder, thus has adverse long-term outcomes in both mental and physical domains of health (Kruesi et al. 2004; Michalska et al. 2015). The diagnosis of CD is established on the basis of DSM-IV criteria and involves direct observation, psychiatric interview and retrospective review (Buitelaar et al. 2013). However, some of the CD symptoms are covert and may be unnoticed and underreported (Buitelaar et al. 2013). Meanwhile, CD can be misdiagnosed by psychiatric clinicians without sufficient experience (Buitelaar et al. 2013).

The etiology and pathogenesis of CD remains unclear. In recent years, neurobiological factors in the etiology of CD have been intensively investigated (Fairchild et al. 2011). Exploring the possible brain abnormalities in CD could help understand the neural basis of CD, and is also an essential step toward developing biomarkers that could improve diagnosis of CD. Structural magnetic resonance imaging (sMRI) has the potential to visualize the whole brain with high spatial resolution and could be used to study brain structure and detect physical abnormalities (Haubold et al. 2012).

Previous sMRI studies have found some brain regions with morphological abnormalities in CD relative to healthy controls (HCs) (Rubia 2011), such as the amygdala (Sterzer et al. 2007), temporal lobes bilaterally (De Brito et al. 2009), anterior

Jianing Zhang and Wanyi Cao contributed equally and the co-first authors.

✉ Shuqiao Yao
shuqiaoyao@163.com

✉ Bingsheng Huang
huangb@szu.edu.cn

[1] School of Biomedical Engineering, Health Science Center, Shenzhen University, Shenzhen, Guangdong, People's Republic of China

[2] Medical Psychological Center, Second Xiangya Hospital, Central South University, Changsha, People's Republic of China

cingulate cortex (Sasayama et al. 2010) and hippocampus (De Brito et al. 2009), however, the results were inconsistent. These studies often used voxel-based morphometry (VBM) to evaluate grey matter (GM) abnormalities in CD. Traditional univariate VBM is a whole-brain, unbiased method for characterizing regional cerebral volume or tissue concentration difference in sMRI images (Ashburner and Friston 2000; Good et al. 2001). It allows for voxel-wise statistical comparison of spatially normalized GM images (Good et al. 2001), which means that each voxel is individually compared. In contrast, multivoxel pattern analysis (MVPA) is a machine learning based pattern classification approach that could decode the distributed (multivoxel) patterns information contained in the brain (Norman et al. 2006). It has been applied to psychiatric disorders' neuroimaging studies in an attempt to avoid the limitation of univariate VBM (Norman et al. 2006). MVPA could detect the spatial information overlooked by VBM. Although VBM could show which brain region differs in either volume or concentration between groups, MVPA could evaluate a set of voxels' classification ability and make inference about patterns of difference by involving the machine learning algorithm (Ashburner 2009; Uddin et al. 2011). Previous studies have reported that MVPA detected the aberrant spatial patterns in different types of psychiatric disorders, such as autism and major depressive disorder (Uddin et al. 2011; Liu et al. 2012). In these studies, MVPA was implemented by using a searchlight algorithm with support vector machine (SVM) (Uddin et al. 2011; Liu et al. 2012).

At present, there have been no MVPA studies focusing on sMRI images of children with CD. The aim of the present study was to characterize the different spatial patterns, which may eventually serve as imaging biomarkers to classify CD from HCs.

## Materials and methods

### Participants

Sixty right-handed male outpatients with CD aging 14~15 years were recruited from the Second Xiangya Hospital of the Central South University (Changsha, Hunan, China). The diagnosis was established by two experienced child psychiatrists using the Structural Clinical Interview for DSM-IV-TR Axis I Disorder-Patient Edition (SCID-I/P). The Barratt Impulsiveness Scale (BIS) was used to measure impulsivity (Yao et al. 2007), which has been broadly used in CD and showed great reliability and validity in previous studies (Stevens and Haney-Caron 2012; Rogers and De Brito 2016). In addition to the total scores, three subtypes of BIS scores were measured: BIS-attention impulsivity, BIS-motor impulsivity and BIS-unplanned impulsivity. The HC group was recruited from the Chinese students in local middle schools. They were interviewed by the same psychiatrists and subjected to SCID-I/P and the Chinese version of the Wechsler Intelligence Scale for Children (C-WISC). Finally, 60 age- and gender-matched students were recruited as the HC group.

The exclusion criteria for both groups were: mental retardation (IQ ≤ 80 on the C-WISC); history of ADHD, or oppositional defiant disorder (ODD); any pervasive developmental or chronic neurological disorder, head trauma, alcohol or substance abuse in the past years; contraindications to MRI. The ethics committee of the Second Xiangya Hospital of the Central South University approved this study. We obtained the written informed consent from each participant and their parents after a complete explanation of the study.

Males only were recruited in the present study. As GM volume changes with different patterns for adolescent males and females, studying mix-gender samples might encounter case-control differences and gender-specific brain differences (Lenroot and Giedd 2006). In addition, it has been reported that males are easier to suffer from CD than females (Dalwani et al. 2015). Thus, we recruited male CD patients only in our current study.

### MRI acquisition

MRI was acquired on a 3-Tesla scanner (Philips Achieva, Amsterdam, Netherlands) at the Second Xiangya Hospital. We acquired T1-weighted three-dimensional magnetization-prepared rapid gradient echo (MPRAGE) images with these parameters: voxel size = $1.0 \times 1.0 \times 1.0$ mm$^3$, repetition time = 8.5 ms, echo time = 3.7 ms, 180 slices, slice thickness = 1 mm, acquisition matrix = $256 \times 256$, field of view = 256 mm × 256 mm, flip angle = 8°. A standard head coil was used for radiofrequency transmission and reception.

### Data preprocessing

The raw DICOM images were converted to NIFTI format using MRIcron (University of South Carolina, Columbia, SC, USA, http://www.mricro.com). The following steps were performed using VBM8 toolbox (http://dbm.neuro.uni-jena.de/vbm) in SPM8 (Version 6313, Wellcome Department of Imaging Neuroscience, London, UK, http://www.fil.ion.ucl.ac.uk/spm) implemented in Matlab R2013a (MathWorks, Natick, Massachusetts). First, all sMRI images were registered to Montreal Neurological Institute (MNI) stereotactic space. Next, the co-registered images were segmented into GM, white matter (WM) and cerebrospinal fluid (CSF) by applying a non-linear deformation. The parameters of non-linear deformation were derived via the high-dimensional Diffeomorphic Anatomical Registration Through Exponentiated Lie Algebra (DARTEL) algorithm and with the predefined templates in VBM8. Then, the segmented images were modulated by using the non-linear deformation

with the purpose of preserving the total volume of each brain tissue. Finally, the images were smoothed with an 8 mm full-width-half-maximum Gaussian kernel.

### MVPA

In this study, MVPA was applied to detect the brain regions discriminating CD from HCs. The input images of MVPA were the smoothed GM images resulted from the data preprocessing step. To perform MVPA, firstly, at each voxel (Vi) of the GM images in the normalized space, a 15 mm-radius sphere centered at Vi was defined. Secondly, we used leave-one-out cross-validation (LOO CV) to split all the input images into the training set (N – 1 subjects; $N = 120$) and the testing set (the remaining subject). The values of all voxels in the sphere defined in the first step were extracted as a high-dimensional feature vector, namely, the so-called "spatial pattern", and used to construct the feature matrix. Thus two feature matrices $M_{F1*S}$ and $M_{F2*S}$ were acquired for the training sets and testing sets (F1 = 119, F2 = 1, S = 687), respectively. F1 and F2 represent the number of subjects in the two sets respectively, whereas S represents the number of voxels in the sphere. Thirdly, the training set was fed into the clasifiers to optimize the model. The classifier used in the classification was linear SVM implemented in LIBSVM toolbox (http://www.csie.ntu.edu.tw/~cjlin/Libsvm). Specifically, 5-fold CV was used to determine the parameter C (regularization) in linear SVM. The training set was divided into five folds, and the parameter that produced the highest accuracy across the five folds were identified as the optimized C. Fourthly, the remaining testing set in the LOO CV was predicted using the optimized C. Finally, the classification accuracy for voxel $V_i$ was obtained by averaging the results at all testing phases in this LOO CV. The resulted three-dimensional accuracy map denotes the classification ability between CD and HCs of all voxels.

Note that the sphere radius in our MVPA method was determined by experience because this is not constant in the former studies (Uddin et al. 2011; Liu et al. 2012). We took into account the balance between computational complexity and spatial pattern information abundance. Given the same stride of sphere, a smaller radius may reduce the computational complexity, however would ignore some spatial information.

To evaluate whether the experimental results were statistically significant, firstly, we supposed a null hypothesis that the output of binary classifier was equally frequent was satisfied (Pereira et al. 2009). Then, the classification of each sample could be modelled as a Bernoulli trial with the probability p (under the null hypothesis, the probability p of success was 0.5) of success, and the three-dimensional accuracy map was assumed to follow the binomial distribution Bi (m, p), with m defined as the number of subjects in the two groups and the probability p equal to 0.5. If we defined k as the number of correctly classified subjects out of m, then the $p$ value was P ($X \geq k$), where X was the random variable. In this way, the three-dimensional accuracy map was converted to a $p$ value map, and if the $p$ value was under a certain threshold, the classification result was considered significant. We used three-dimensional connected domain algorithm implemented in Matlab R2013a to construct the clusters, and the cluster of significant difference was defined if the cluster contained at least 50 adjacent voxels with uncorrected $p < 0.0001$ (Uddin et al. 2011).

In order to build classification models with the detected spatial patterns, we selected all the voxel values contained in the clusters defined above as the input features of SVM with linear kernel. The performance of the classification models was evaluated using the receiver operating characteristic (ROC) curve. We also calculated the accuracy, specificity and sensitivity from the ROC curve by the decision threshold with the highest accuracy. The area under ROC curve (AUC) was also obtained.

### Statistical analysis

Two sample t-test was performed to determine if the means of CD and HCs in age, IQ, BIS features were different at the typical significance level. Besides, Pearson correlation was used to explore the association between volumes in the detected clusters and IQ, BIS-attention impulsivity, BIS-motor impulsivity, BIS-unplanned impulsivity and BIS-total scores.

## Results

### Demographic and clinical variables

Table 1 lists the demographic characteristics of all subjects. No significant difference was found in age between the two groups ($p = 0.214$). Compared with the HC group, IQ was significantly lower in CD group ($p < 0.001$). CD group had significantly more severe BIS-motor impulsivity ($p < 0.001$), BIS-unplanned impulsivity ($p = 0.001$) and BIS-total scores ($p < 0.001$) than the HC group. BIS-attention impulsivity of CD group was higher than that of the HC group, however the difference was insignificant ($p = 0.481$).

### MVPA

As summarized in Table 2 and displayed in Figs. 1, 7 cortical and subcortical regions showed high classification accuracy with GM differences between CD and HCs, including the cerebellum posterior lobe, temporal lobe, parahippocampal gyrus, lingual gyrus, insula, parietal lobe and medial frontal gyrus. GM in these brain regions discriminated CD with peak accuracy of up to 83%. Using the spatial patterns as input

**Table 1** Demographic and clinical characteristics of the CD group and the HC group

| Measure | CD | HCs | *p* Value |
|---|---|---|---|
| Age in years | 15.3(1.0) | 15.5(0.7) | 0.214 |
| IQ | 97.0(12.3) | 105.4(8.8) | <0.001 |
| BIS-attention impulsivity | 18.5(3.2) | 18.1(3.1) | 0.481 |
| BIS-motor impulsivity | 26.2(5.0) | 22.4(3.8) | <0.001 |
| BIS-unplanned impulsivity | 31.1(4.6) | 28.4(3.7) | 0.001 |
| BIS-total scores | 75.8(10.9) | 69.0(8.1) | <0.001 |

Data are given as mean (standard deviation). Two sample t-test was performed to determine if the means of CD and HCs in age, IQ, BIS features are different at the typical significance level. CD, conduct disorder; HCs, healthy controls; IQ, Intelligence Quotient; BIS, Barratt Impulsiveness Scale.

features and 5-fold CV, SVM with linear kernel achieved AUC of 0.74, accuracy of 71.7%, specificity of 65.0%, and sensitivity of 78.3%.

### Correlation analysis

We did not find significant correlations between cluster volume and IQ. As shown in Tables 3 and 4, significant correlations were observed between the volumes of some clusters and BIS scores. However, these correlations were moderate with relatively low coefficients and did not survive Bonferroni correction (corrected significance threshold of 0.05/28).

## Discussion

In the current study, we have shown that sMRI with MVPA might be a useful and reliable approach to study the neuroanatomical changes to differentiate CD from HCs, by which we detected 7 cortical and subcortical regions with GM differences between CD and HCs, including the cerebellum posterior lobe, temporal lobe, parahippocampal gyrus, lingual gyrus, insula, parietal lobe and medial frontal gyrus. GM in these brain regions discriminated CD with peak accuracy of up to 83%, which was better than our previous VBM study (Zhang et al. 2018). The results indicated that the abnormal neuroanatomical structures of CD were mainly involved in the frontal, temporal, parietal and occipital regions as well as cerebellum.

We achieved high classification accuracy with GM in the cerebellum, including the cerebellum posterior lobe and cerebellum anterior lobe. Several previous studies in CD have shown GM deficits in the cerebellum (Stevens and Haney-Caron 2012; Huebner et al. 2008; Bussing et al. 2002). As a part of the fronto-striato-cerebellar brain circuit, cerebellum plays an important role in the inhibitory control and behavioral regulation (Dalwani et al. 2011; Arnsten and Rubia 2012). Cerebellum also has been reported to be important for cool executive function, which encompasses inhibition, planning, and the ability to creatively generate solutions for problems (Rubia 2011). Therefore, deficits in the cerebellum may be correlated with impulsive behavior in CD. Recently several functional MRI studies have also reported cerebellum abnormality in patients of CD. During the sustained attention task performance, CD showed decreased cerebellum activation compared with attention deficit hyperactivity disorder and HCs (Rubia et al. 2009); and decreased regional homogeneity in anterior cerebellum and posterior cerebellum (Wu et al. 2017). Our results showed that increased impulsivity was significantly correlated with the decreased volume of cerebellum posterior lobe, indicating that the cerebellum posterior lobe may regulate impulsivity. Cerebellum posterior lobe dysfunction probably lead to the behavioral disinhibition associated with impulsivity of CD. All the above-mentioned studies have demonstrated that cerebellum plays a crucial role in the pathophysiology of CD. The high classification accuracy of the cerebellum in our study may be explained by the cerebellar deficits and dysfunction in CD reported in these previous studies.

The right temporal lobe also showed high classification accuracy. This can also be explained by the previous studies which have reported GM abnormalities in the temporal lobe of antisocial individuals (Kruesi et al. 2004; De Brito et al. 2009; Sasayama et al. 2010; Huebner et al. 2008; Barkataki et al. 2006; Muller et al. 2008). The temporal lobe is one of the major brain areas associated with antisocial and aggressive behavior (Raine 2013; Raine and Yang 2006; Hyatt et al. 2012). Decreased GM volume of the temporal lobe was observed in children and adolescents with CD compared with HCs (Kruesi et al. 2004; Huebner et al. 2008). In contrast, one study reported increased GM volume in boys with CD (De Brito et al. 2009). They selected only boys with callous-unemotional conduct problems and used hyperactivity in attention symptoms as a covariate (De Brito et al. 2009). The inconsistency of the results may be caused by the different control for important factors such as cognitive ability and age range.

In addition to the cerebellum and temporal lobe, GM in insula also allowed for high classification accuracy. Anterior insular cortex, as a part of the insular cortex, is known to be involved in emotion processing and coordination of appropriate responses to events (Craig 2002). Abnormal GM volume in insula has been found in CD (Sterzer et al. 2007; Gasquoine 2014). Dysfunction in CD in the insula may result from the decreased ability to learn from, as well as avoid, risky situation and negative consequences when prompted by internal emotional states (Hyatt et al. 2012). A structural deficit in the anterior insular cortex is related to the impaired capacity of empathy and aberrant social behavior in CD (Sterzer et al. 2007). Recently, two previous fMRI studies suggested that

**Table 2** Grey matter differences between CD group and HC group

| Region (Hemisphere) | Cluster size (voxels) | MNI coordinates | | | Peak accuracy (%) |
|---|---|---|---|---|---|
| | | X | Y | Z | |
| Uvula/Cerebellum posterior lobe (L) | 335 | −21 | −80 | −32 | 83 |
| Temporal lobe/Cerebellum anterior lobe (R) | 219 | 38 | −53 | −33 | 76 |
| Parahippocampal Gyrus/Cerebellum anterior lobe (R) | 98 | 26 | −50 | −20 | 81 |
| Occipital lobe/Lingual gyrus (L) | 57 | −24 | −89 | −9 | 76 |
| Insula (R) | 96 | 41 | −17 | 5 | 78 |
| Parietal Lobe/Supramarginal Gyrus (R) | 250 | 59 | −45 | 30 | 78 |
| Frontal Lobe/Superior Frontal Gyrus/Medial Frontal Gyrus (L) | 165 | −9 | 48 | 33 | 78 |

The peak accuracy of each cluster was calculated as the maximum of cross-validation accuracy in this cluster.

*CD* conduct disorder; *HCs* healthy controls; *L* left hemisphere; *R* right hemisphere

the lower amplitude of low-frequency fluctuations in insula was observed in adolescents with CD (Zhou et al. 2015), and activities in anterior insula were negatively correlated with response to viewing others being harmed in CD symptoms (Michalska et al. 2016). A study found a positive correlation between regional homogeneity in the insula and BIS scores in the CD patients (Wu et al. 2017; Jiang et al. 2015). Higher BIS-attention impulsivity scores indicated greater attention impulsivity, a crucial feature of CD. Therefore, in our results, the positive correlation between volume in the insula and BIS-attention impulsivity scores may reflect the close relationship between abnormity in the insula and attention impulsivity. These may explain the high classification accuracy of the insula in our study.

We also discovered high classification accuracy in several other brain regions, including lingual gyrus, supramarginal gyrus, superior frontal gyrus and medial frontal gyrus. According to some previous neuroimaging studies of CD, These brain regions have shown abnormality in CD (Stevens and Haney-Caron 2012; Rogers and De Brito 2016; Dalwani et al. 2011; Lu et al. 2015). Specifically, left lingual gyrus, as part of the medial visual network, is expected to be relevant to perceptual systems responsible for perceptual dysfunction in male adolescents with CD (Lu et al. 2015). Another study using female CD patients as participants also reported reduced GM volume in the left lingual gyrus (Budhiraja et al. 2017). Volume in lingual gyrus showed a positive correlation with BIS-unplanned impulsivity. Right supramarginal gyrus, as a part of the inferior parietal cortex, is important in the social judgment situation, and damage of supramarginal gyrus can cause disorders accompanied with distorted body knowledge and self-awareness (Silani et al. 2013; Berlucchi and Aglioti 1997). In a task of fairness decisions in response to emotions, the CD boys showed less activation in supramarginal gyrus when receiving positive compared with negative emotional reactions (Klapwijk et al. 2016). The frontal lobe may be closely related to social behavior (Kruesi et al. 2004). It has been reported that CD had significantly reduced GM volume in the left medial and superior frontal gyrus, which was essential for social cognition and perspective taking (Rogers and De Brito 2016). The high classification accuracy in lingual gyrus, supramarginal gyrus, and frontal lobe may be explained by these former studies of CD.

Several structural and functional imaging studies of CD found that CD was associated with abnormalities of the paralimbic system, including the insula, hippocampus and

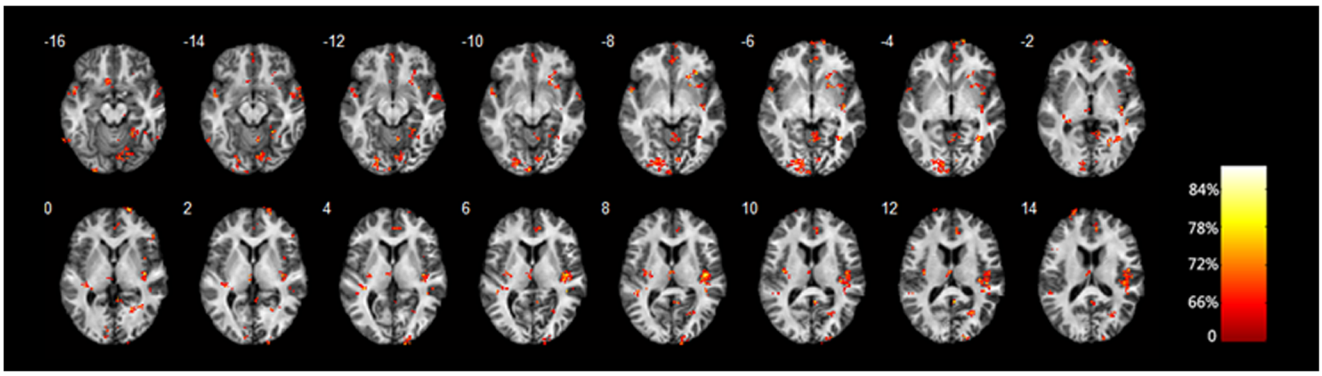


**Fig. 1** Results of MVPA presented at a $p$ value less than 0.0001 and extent threshold of 50 adjacent voxels. Colors symbolize the accuracy of $V_i$ (see colorbar) in classifying CD from HCs

**Table 3** Correlations between the clusters volume of CD and BIS scores

| Region (Hemisphere) | BIS-attention impulsivity | BIS-motor impulsivity | BIS-unplanned impulsivity | BIS-total scores |
|---|---|---|---|---|
| Uvula/Cerebellum Posterior Lobe (L) | −0.17(0.214) | −0.36(**0.008****) | −0.29(**0.036***) | −0.34(**0.013***) |
| Temporal Lobe/Cerebellum Anterior Lobe (R) | −0.03(0.849) | −0.11(0.417) | −0.16(0.244) | −0.11(0.425) |
| Parahippocampal Gyrus/Cerebellum Anterior Lobe (R) | 0.10(0.480) | −0.05(0.702) | −0.06(0.656) | −0.02(0.880) |
| Occipital Lobe/Lingual Gyrus (L) | 0.13(0.346) | −0.04(0.802) | 0.22(0.116) | 0.11(0.422) |
| Insula (R) | 0.19(0.173) | 0.14(0.327) | 0.04(0.796) | 0.14(0.335) |
| Parietal Lobe/Supramarginal Gyrus (R) | 0.00(0.984) | −0.09(0.513) | −0.15(0.282) | −0.10(0.459) |
| Frontal Lobe/Superior Frontal Gyrus/Medial Frontal Gyrus (L) | 0.26(0.058) | 0.22(0.875) | 0.06(0.683) | 0.11(0.425) |

** $p < 0.01$, * $p < 0.05$. CD, conduct disorder; BIS, Barratt Impulsiveness Scale

superior temporal lobes (Arnsten and Rubia 2012; Mohanty et al. 2008; Rubia et al. 2008; Decety et al. 2009). The limbic system and underlying subcortical brain areas play a critical role in the processing of motivation and affect (Rubia 2011). It is likely that deficits in the limbic system are relevant to antisocial pathology (Huebner et al. 2008). Cortical thinning of paralimbic structures has been identified in CD subjects versus HCs. Furthermore, abnormality of the paralimbic system reflects a non-specific effect of the early-onset CD and adolescent-onset CD (Jiang et al. 2015). All the above studies could further explain the high classification accuracy in these brain regions.

The present study also revealed significant correlations between volumes in some detected clusters and BIS scores. The correlation analysis results suggested that the volumes of left cerebellum posterior lobe and right insula were associated with behavioral and clinical variables. Previous studies have demonstrated a negative correlation between CD symptoms and right insula volume (Fairchild et al. 2011; Huebner et al. 2008). However, the correlation were moderate with relatively low coefficients.

In order to evaluate the different performance by MVPA and VBM analysis, we compared the results of MVPA and our former study based on VBM (Zhang et al. 2018). By VBM, the decrease in GM volume of CD patients was observed mainly in the cerebellum posterior lobe, the inferior parietal lobule and insula, while the increase was mainly in the medial frontal gyrus, the superior frontal gyrus and anterior cingulate (Zhang et al. 2018). With MVPA, we also in addition detected the lingual gyrus and supramarginal gyrus, which were important brain regions associated with CD (Lu et al. 2015; Budhiraja et al. 2017; Klapwijk et al. 2016). This may suggest that MVPA results were more consistent with the former studies, and VBM might not be sensitive enough to detect the subtle differences between the two groups. The different results between the two methods can be explained by the difference in feature extraction. VBM performs two sample t-test voxel by voxel between groups. In MVPA, the features used were all voxels' values of the sphere, which not only have one-dimensional greyscale value information, but also include three-dimensional spatial pattern information. Therefore, the features in MVPA may contain more spatial patterns' information compared with VBM.

There are several limitations in the present study. Firstly, sample size is an important issue, but currently we have not found studies investigating the effect of sample size. Although the feature extraction procedures were different between VBM and MVPA, the preprocessing steps and classifiers were the same. For VBM, we have tested the robustness of classification models under different circumstance, such as different classifiers, and found that with the same sample size as in our

**Table 4** Correlations between the clusters volume of HCs and BIS scores

| Region (Hemisphere) | BIS-attention impulsivity | BIS-motor impulsivity | BIS-unplanned impulsivity | BIS-total scores |
|---|---|---|---|---|
| Uvula/Cerebellum posterior lobe (L) | −0.10(0.459) | −0.10(0.440) | −002(0.855) | −0.10(0.467) |
| Temporal Lobe/Cerebellum anterior lobe (R) | −0.05(0.691) | −0.01(0.947) | −0.14(0.296) | −0.09(0.513) |
| Parahippocampal Gyrus/Cerebellum anterior lobe (R) | −0.04(0.765) | −0.06(0.640) | −0.14(0.312) | −0.11(0.430) |
| Occipital Lobe/Lingual gyrus (L) | −0.04(0.763) | 0.01(0.957) | 0.17(0.205) | 0.06(0.633) |
| Insula (R) | 0.27(**0.039***) | 0.27(**0.039***) | 0.01(0.958) | 0.23(0.077) |
| Parietal Lobe/Supramarginal Gyrus (R) | −0.17(0.214) | 0.06(0.675) | −0.05(0.711) | −0.06(0.655) |
| Frontal lobe/Superior frontal Gyrus/Medial frontal gyrus (L) | −0.10(0.485) | −0.08(0.547) | −0.09(0.515) | −0.11(0.398) |

*$p < 0.05$. HCs, healthy controls; BIS, Barratt Impulsiveness Scale

present study we achieved stable results (Zhang et al. 2018). These results indicated the sample size was appropriate in our study. However, the robustness of the findings requires further validation in a clinical cohort that adequately represents the target patient population, especially the use of prospectively collected data is desirable (Park and Han 2018), thus we consider that our sample size may not be large and representative enough. In further studies, the current result should be validated with a larger and more heterogeneous cohort. Secondly, there are some limitations in our MVPA method. For example, some hyperparameters such as the radius and step of the sphere were defined based on experience. We chose one voxel as the stride in MVPA to make sure that no spatial pattern information was ignored, however, the time cost of MVPA computation was then expensive. Studies should be done to search for better hyperparameters in MVPA. Finally, although our approach could identify some structural features of CD, the sMRI spatial pattern may not be sufficient enough for better classification. Multimodality studies including functional MRI may be performed to explore better classification of CD from HCs.

## Conclusion

Our MVPA study found that multiple brain regions, including the cerebellum posterior lobe, temporal lobe, parahippocampal gyrus, lingual gyrus, insula, parietal lobe and medial frontal gyrus, exhibited aberrant structural spatial patterns in CD. These findings, derived from sMRI and consistent with previous findings, may contribute to the identification of the neuroanatomical changes differentiating CD from HCs. This MVPA approach might also be useful for the development of targeted early interventions for CD.

**Acknowledgements** The study was funded by the Natural Science Foundation of China (No. 81471384) and the Seed Funding from Scientific and Technical Innovation Council of Shenzhen Government (No. 000048).

### Compliance with ethical standards

**Financial disclosures** None of the authors has any conflicts of interest to disclosure. We confirm that we have read the Journal's position on issues involved in ethical publication and affirm that this report is consistent with those guidelines.

## References

Arnsten, A. F., & Rubia, K. (2012). Neurobiological circuits regulating attention, cognitive control, motivation, and emotion: Disruptions in neurodevelopmental psychiatric disorders [J]. *Journal of the American Academy of Child and Adolescent Psychiatry, 51*(4), 356–367.

Ashburner, J. (2009). Computational anatomy with the SPM software [J]. *Magnetic Resonance Imaging, 27*(8), 1163–1174.

Ashburner, J., & Friston, K. (2000). Voxel-based morphometry—The methods [J]. *Neuroimage, 11*(6 Pt 1), 805–821.

Barkataki, I., Kumari, V., Das, M., Taylor, P., & Sharma, T. (2006). Volumetric structural brain abnormalities in men with schizophrenia or antisocial personality disorder [J]. *Behavioural Brain Research, 169*(2), 239–247.

Berlucchi, G., & Aglioti, S. (1997). The body in the brain: Neural bases of corporeal awareness [J]. *Trends in Neurosciences, 20*(12), 560–564.

Budhiraja, M., Savic, I., Lindner, P., Jokinen, J., Tiihonen, J., & Hodgins, S. (2017). Brain structure abnormalities in young women who presented conduct disorder in childhood/adolescence [J]. *Cognitive, Affective, & Behavioral Neuroscience, 17*(4), 869–885.

Buitelaar, J. K., Smeets, K. C., Herpers, P., Scheepers, F., Glennon, J., & Rommelse, N. N. J. (2013). Conduct disorders [J]. *European Child & Adolescent Psychiatry, 22*(1), 49–54.

Bussing, R., Grudnik, J., Mason, D., Wasiak, M., & Leonard, C. (2002). ADHD and conduct disorder: An MRI study in a community sample [J]. *The World Journal of Biological Psychiatry, 3*(4), 216–220.

Cappadocia, M. C., Desrocher, M., Pepler, D., & Schroeder, J. H. (2009). Contextualizing the neurobiology of conduct disorder in an emotion dysregulation framework [J]. *Clinical Psychology Review, 29*(6), 506–518.

Craig, A. D. (2002). How do you feel? Interoception: The sense of the physiological condition of the body [J]. *Nature Reviews. Neuroscience, 3*(8), 655–666.

Dalwani, M., Sakai, J. T., Mikulich-Gilbertson, S. K., Tanabe, J., Raymond, K., McWilliams, S. K., Thompson, L. L., Banich, M. T., & Crowley, T. J. (2011). Reduced cortical gray matter volume in male adolescents with substance and conduct problems [J]. *Drug and Alcohol Dependence, 118*(2–3), 295–305.

Dalwani, M. S., McMahon, M. A., Mikulich-Gilbertson, S. K., Young, S. E., Regner, M. F., Raymond, K. M., McWilliams, S. K., Banich, M. T., Tanabe, J. L., Crowley, T. J., & Sakai, J. T. (2015). Female adolescents with severe substance and conduct problems have substantially less brain gray matter volume [J]. *PLoS One, 10*(5), e0126368.

De Brito, S. A., et al. (2009). Size matters: Increased grey matter in boys with conduct problems and callous-unemotional traits [J]. *Brain, 132*(Pt 4), 843–852.

Decety, J., Michalska, K. J., Akitsuki, Y., & Lahey, B. B. (2009). Atypical empathic responses in adolescents with aggressive conduct disorder: A functional MRI investigation [J]. *Biological Psychology, 80*(2), 203–211.

Fairchild, G., Passamonti, L., Hurford, G., Hagan, C. C., von dem Hagen, E. A. H., van Goozen, S. H. M., Goodyer, I. M., & Calder, A. J. (2011). Brain structure abnormalities in early-onset and adolescent-onset conduct disorder [J]. *The American Journal of Psychiatry, 168*(6), 624–633.

Gasquoine, P. G. (2014). Contributions of the insula to cognition and emotion [J]. *Neuropsychology Review, 24*(2), 77–87.

Good, C. D., Johnsrude, I. S., Ashburner, J., Henson, R. N. A., Friston, K. J., & Frackowiak, R. S. J. (2001). A voxel-based morphometric study of ageing in 465 normal adult human brains [J]. *NeuroImage, 14*(1), 21–36.

Haubold, A., Peterson, B. S., & Bansal, R. (2012). Annual research review: Progress in using brain morphometry as a clinical tool for diagnosing psychiatric disorders [J]. *Journal of Child Psychology and Psychiatry, 53*(5), 519–535.

Huebner, T., et al. (2008). Morphometric brain abnormalities in boys with conduct disorder [J]. *Journal of the American Academy of Child and Adolescent Psychiatry, 47*(5), 540–547.

Hyatt, C. J., Haney-Caron, E., & Stevens, M. C. (2012). Cortical thickness and folding deficits in conduct-disordered adolescents [J]. *Biological Psychiatry, 72*(3), 207–214.

Jiang, Y., Guo, X., Zhang, J., Gao, J., Wang, X., Situ, W., Yi, J., Zhang, X., Zhu, X., Yao, S., & Huang, B. (2015). Abnormalities of cortical structures in adolescent-onset conduct disorder [J]. *Psychological Medicine, 45*(16), 3467–3479.

Klapwijk, E. T., Lelieveld, G. J., Aghajani, M., Boon, A. E., van der Wee, N. J. A., Popma, A., Vermeiren, R. R. J. M., & Colins, O. F. (2016). Fairness decisions in response to emotions: A functional MRI study among criminal justice-involved boys with conduct disorder [J]. *Social Cognitive and Affective Neuroscience, 11*(4), 674–682.

Kruesi, M. J., et al. (2004). Reduced temporal lobe volume in early onset conduct disorder [J]. *Psychiatry Research, 132*(1), 1–11.

Lenroot, R. K., & Giedd, J. N. (2006). Brain development in children and adolescents: Insights from anatomical magnetic resonance imaging [J]. *Neuroscience & Biobehavioral Reviews, 30*(6), 718–729.

Liu, F., Guo, W., Yu, D., Gao, Q., Gao, K., Xue, Z., du, H., Zhang, J., Tan, C., Liu, Z., Zhao, J., & Chen, H. (2012). Classification of different therapeutic responses of major depressive disorder with multivariate pattern analysis method based on structural MR scans [J]. *PLoS One, 7*(7), e40968.

Lu, F.-M., Zhou, J. S., Zhang, J., Xiang, Y. T., Zhang, J., Liu, Q., Wang, X. P., & Yuan, Z. (2015). Functional connectivity estimated from resting-state fMRI reveals selective alterations in male adolescents with pure conduct disorder [J]. *PLoS One, 10*(12), e0145668.

Michalska, K. J., Decety, J., Zeffiro, T. A., & Lahey, B. B. (2015). Association of regional gray matter volumes in the brain with disruptive behavior disorders in male and female children [J]. *Neuroimage Clin, 7*, 252–257.

Michalska, K. J., Zeffiro, T. A., & Decety, J. (2016). Brain response to viewing others being harmed in children with conduct disorder symptoms [J]. *Journal of Child Psychology and Psychiatry, 57*(4), 510–519.

Mohanty, A., et al. (2008). The Spatial Attention Network Interacts with Limbic and Monoaminergic Systems to Modulate Motivation-Induced Attention Shifts [J]. *Cerebral Cortex (New York, NY), 18*(11), 2604–2613.

Muller, J. L., et al. (2008). Gray matter changes in right superior temporal gyrus in criminal psychopaths. Evidence from voxel-based morphometry [J]. *Psychiatry Research, 163*(3), 213–222.

Norman, K. A., Polyn, S. M., Detre, G. J., & Haxby, J. V. (2006). Beyond mind-reading: Multi-voxel pattern analysis of fMRI data [J]. *Trends in Cognitive Sciences, 10*(9), 424–430.

Park, S. H., & Han, K. (2018). Methodologic guide for evaluating clinical performance and effect of artificial intelligence Technology for Medical Diagnosis and Prediction [J]. *Radiology, 286*(3), 171920.

Pereira, F., Mitchell, T., & Botvinick, M. (2009). Machine learning classifiers and fMRI: A tutorial overview [J]. *Neuroimage, 45*(1 Suppl), S199–S209.

Raine A, The psychopathology of crime: Criminal behavior as a clinical disorder [M]. Elsevier 2013.

Raine, A., & Yang, Y. (2006). Neural foundations to moral reasoning and antisocial behavior [J]. *Social Cognitive and Affective Neuroscience, 1*(3), 203–213.

Rogers, J. C., & De Brito, S. A. (2016). Cortical and subcortical gray matter volume in youths with conduct problems: A meta-analysis [J]. *JAMA Psychiatry, 73*(1), 64–72.

Rubia, K. (2011). Cool inferior frontostriatal dysfunction in attention-deficit/hyperactivity disorder versus "hot" ventromedial orbitofrontal-limbic dysfunction in conduct disorder: A review [J]. *Biological Psychiatry, 69*(12), e69–e87.

Rubia, K., et al. (2008). Dissociated functional brain abnormalities of inhibition in boys with pure conduct disorder and in boys with pure attention deficit hyperactivity disorder [J]. *The American Journal of Psychiatry, 165*(7), 889–897.

Rubia, K., et al. (2009). Disorder-specific dissociation of orbitofrontal dysfunction in boys with pure conduct disorder during reward and ventrolateral prefrontal dysfunction in boys with pure ADHD during sustained attention [J]. *The American Journal of Psychiatry, 166*(1), 83–94.

Sasayama, D., Hayashida, A., Yamasue, H., Harada, Y., Kaneko, T., Kasai, K., Washizuka, S., & Amano, N. (2010). Neuroanatomical correlates of attention-deficit-hyperactivity disorder accounting for comorbid oppositional defiant disorder and conduct disorder [J]. *Psychiatry and Clinical Neurosciences, 64*(4), 394–402.

Silani, G., Lamm, C., Ruff, C. C., & Singer, T. (2013). Right supramarginal gyrus is crucial to overcome emotional egocentricity bias in social judgments [J]. *The Journal of Neuroscience, 33*(39), 15466–15476.

Sterzer, P., Stadler, C., Poustka, F., & Kleinschmidt, A. (2007). A structural neural deficit in adolescents with conduct disorder and its association with lack of empathy [J]. *Neuroimage, 37*(1), 335–342.

Stevens, M. C., & Haney-Caron, E. (2012). Comparison of brain volume abnormalities between ADHD and conduct disorder in adolescence [J]. *Journal of Psychiatry & Neuroscience: JPN, 37*(6), 389–398.

Uddin, L. Q., Menon, V., Young, C. B., Ryali, S., Chen, T., Khouzam, A., Minshew, N. J., & Hardan, A. Y. (2011). Multivariate searchlight classification of structural magnetic resonance imaging in children and adolescents with autism [J]. *Biological Psychiatry, 70*(9), 833–841.

Wu, Q., Zhang, X., Dong, D., Wang, X., & Yao, S. (2017). Altered spontaneous brain activity in adolescent boys with pure conduct disorder revealed by regional homogeneity analysis [J]. *European Child & Adolescent Psychiatry, 26*(7), 827–837.

Yao, S., Yang, H., Zhu, X., Auerbach, R. P., Abela, J. R. Z., Pulleyblank, R. W., & Tong, X. (2007). An examination of the psychometric properties of the Chinese version of the Barratt impulsiveness scale, 11th version in a sample of Chinese adolescents [J]. *Perceptual and Motor Skills, 104*(3 Pt 2), 1169–1182.

Zhang, J., et al. (2018). Distinguishing Adolescents With Conduct Disorder From Typically Developing Youngsters Based on Pattern Classification of Brain Structural MRI [J]. *Frontiers in Human Neuroscience, 12*(152).

Zhou, J., Yao, N., Fairchild, G., Zhang, Y., & Wang, X. (2015). Altered hemodynamic activity in conduct disorder: A resting-state FMRI investigation [J]. *PLoS One, 10*(3), e0122750.